

# Physical Testing for Wind Resistance of Retrofit Single-Ply Roof Systems Over Structural Metal Panel Roof Systems

**James R. Kirby, AIA**  
**Jennifer Keegan, AAIA**

*GAF*

809 Redbud Lane, Wilmette, IL 60091  
312-505-6630 • james.kirby@gaf.com

**Mohamed ElGawady, PhD**  
**Yasser Darwish**

*Missouri University of Science and Technology*

1401 N. Pine St., Rolla, MO 65409-6510  
573-341-6947 • elgawadym@mst.edu



International Institute of  
Building Enclosure Consultants

**IIBEC 2020 Virtual International  
Convention and Trade Show  
June 12-14, 2020**

# ABSTRACT

Retrofit single-ply roof systems (RSPRSs) are increasingly being used to re-cover existing structural metal panel roofs. One of the primary concerns when an RSPRS is installed over a structural metal panel roof is wind uplift. Of significant concern is when an RSPRS is mechanically fastened into every other purlin instead of every purlin. The every-other method of installation changes the wind resistance load path of the metal building. This every-other load path seemingly doubles the load on the purlin-to-mainframe connection for the purlins to which the RSPRS is attached.

ASTM E1592 physical testing was performed on three test roof assemblies—each consisting of a mechanically attached TPO with flat stock and flute-fill polyisocyanurate over a 24-in.-wide structural metal panel roof system. Each RSPRS had different fastener patterns, which resulted in different wind uplift resistance values. The tests were heavily monitored to obtain deflection measurements and stress/strain information for multiple components within the assembly.

The results from an analysis of the three physical tests will be presented. The results from physical testing (small and large scale) were used to develop finite element analysis (FEA) modeling of alternative fastening patterns, and these conclusions will be presented.

# SPEAKERS



**James R. Kirby** holds a master of architecture degree with a structures option, and is a licensed architect concentrating on building and roofing science. He has over 25 years of experience in the roofing industry, covering low-slope, steep-slope, metal, SPF, vegetative, and rooftop photovoltaics. He understands the effects of heat, air, and moisture on a roof system. Kirby presents building and roofing science information to architects, consultants, and building owners, and he publishes articles and blogs for building owners and facility managers and the roofing industry at large. He is a member of AIA, ASTM, ICC, MRCA, NRCA, and IIBEC.



**Mohamed A. ElGawady, PhD**, is a professor and Benavides Faculty Scholar at Missouri University of Science and Technology (formerly University of Missouri-Rolla) with 20 years of experience in extreme loading and sustainability.

# Physical Testing for Wind Resistance of Retrofit Single-Ply Roof Systems Over Structural Metal Panel Roof Systems

## INTRODUCTION

Retrofit single-ply roof systems (RSPRSs) are increasingly being used to recover existing structural metal panel roofs.<sup>1</sup> One of the primary concerns when an RSPRS is installed over a structural metal panel roof is wind uplift performance of the retrofit roof system. Currently, RSPRSs can be attached with different fastening approaches: into the pan, into every purlin, and into every other purlin. Fastener densities also vary, and there have been no publicly available validation studies or data supporting any particular approach. Non-validated attachment methods could result in failures during wind events. Therefore, the objective of this research is to determine the wind uplift resistance of an RSPRS installed over existing structural metal panel roof systems fastened directly into purlins.

A variety of fastening patterns and fastener densities have been studied in order to provide a better understanding of the effect of wind loads on these systems. Of significant concern is when an RSPRS is mechanically fastened into every other purlin instead of every purlin. The every-other type of installation changes the wind resistance load path of the metal building. The every-other load path theoretically doubles the load on the purlin-to-mainframe connection for the purlins to which the RSPRS is attached. This study was designed to evaluate these concerns.

## EXPERIMENTAL APPROACH

ASTM E1592<sup>2</sup> physical testing was performed on four test roof assemblies, each consisting of a mechanically attached or induction-welded TPO membrane directly fastened into the purlins that support the structural metal roof panels. Each system included flute-fill insulation and flat-stock insulation over the 24-in.-wide structural metal roof panels with double-lock stand-

ing seams. The structural metal panels were attached to purlins using expansion clips screwed to the purlins. Each of the four RSPRSs had a different membrane fastening pattern, which resulted in different wind uplift resistance values. The tests were monitored to obtain deflection measurements and strain values for multiple components, including the TPO membrane, clips, and panels within each of the RSPRS assemblies.

The results from the physical testing and wind uplift resistance of the four physical tests are presented in this paper. The results from physical testing (small- and large-scale) are used to develop finite element analysis modeling of alternative fastening patterns.

## Test Chamber

A 10-ft.-wide x 20-ft.-long x 24-in.-tall steel chamber was constructed to be the vacuum chamber. This consisted of two 12-in.-deep C-channels stacked and covered by steel plates and external stiffener members. The vacuum chamber rested directly on the test roofs and was used to provide negative pressure to simulate uplift forces.

## Test Roof Construction

Four full-scale test roofs were constructed and tested. The test roofs were installed by Missouri Builder Services<sup>4</sup> with oversight by the lead author of this paper. The test roofs were constructed on January 9, March 26, April 25, and July 1,



Fastener densities also vary, and there have been no publicly available validation studies or data supporting any particular approach. Non-validated attachment methods could result in failures during wind events.



## TEST APPARATUS AND TEST ROOFS

The physical testing was performed at the Civil, Architectural and Environmental Engineering Department at the Missouri University of Science and Technology<sup>3</sup> (MS&T).

2019. After the test roofs were constructed, the MS&T research team instrumented the assemblies for data collection. See the Data Collection section for additional information. The test roofs were tested on February 5, April 3, May 10, and July 9, 2019.

The test roofs were constructed on site on a raised platform in order to accommodate measuring instrumentation for



**Figure 1 – The as-built chamber for Test #3.**

data collection. *Figure 1* shows the as-built E1592 physical testing chamber; it is supported by four columns.

### Structural Metal Panel Roof System

The four test roofs consisted of 24-in.-wide, 24-gauge structural metal roof panels attached to 16-gauge Z-purlins. The structural metal panels were connected to the purlins with concealed expansion clips and purlin screws manufactured by the roof panel manufacturer. The purlins were connected to and supported by horizontal steel channels; the purlin/channel construction was supported by four vertical steel columns. Each test used new materials for all roof system components; no components were reused.

The double-lock metal panel seams for Test #1 were constructed using the manufacturer’s recommended hand-seaming tool, which was determined to be overly labor-intensive and time-consuming. The double-lock metal panel seams for Tests #2, #3, and #4 were installed using the manufacturer’s automatic seaming tool.

The female leg on the first panel and the male leg of the fifth panel

had approximately 1½ in. of the trapezoidal portion removed to allow the panels to be nested under the upper flange of the C-channel. At the purlin locations, the outer edges of each of the cut panels were secured to the purlins with the same screws used to attach the clips to the purlins. At both ends, the metal panels were secured to the purlins with two screws in each panel.

were mechanically attached to the pans of the metal panels to reduce shifting of the insulation during testing and to match existing field practices. *Table 1* provides a summary of the seaming method, flute-fill insulation, and membrane fastener type for each of the test roofs.

A minimal number of fasteners was used to secure all layers of insulation; insulation fastener placement is not critical to

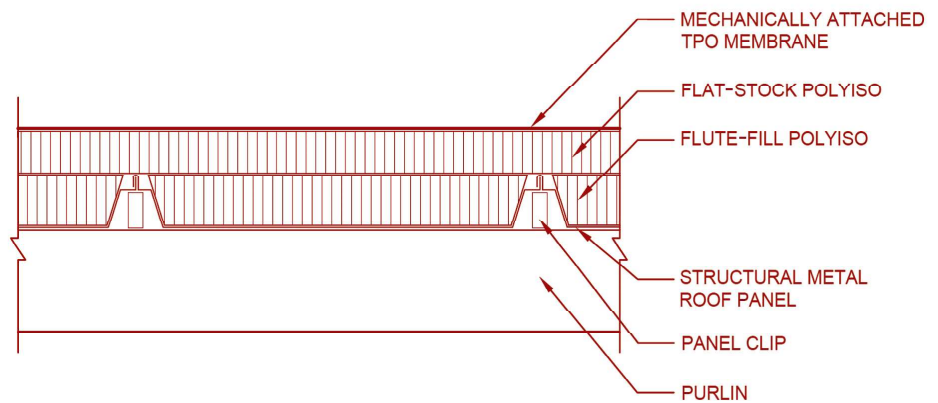


**Figure 2 – Cross section of the RSPRS over a structural metal panel roof system.**

| Test Roof # | Seaming Method | Flute Fill Insulation | Membrane Fastener            |
|-------------|----------------|-----------------------|------------------------------|
| 1           | Hand           | Two 2-in. layers      | 2¾-in. barbed plate          |
| 2           | Automatic      | One 3-in. layer       | 2¾-in. barbed plate          |
| 3           | Automatic      | One 3-in. layer       | 2¾-in. barbed plate          |
| 4           | Automatic      | One 3-in. layer       | 3-in. induction-welded plate |

**Table 1 – Summary of seaming method, flute-fill insulation, and membrane fastener type.**

the wind uplift resistance of the test roofs.

A 60-mil TPO membrane was installed over the insulation for each test. Details of the four distinct TPO installations are provided in the next section. *Figure 3* shows the installed TPO for Test #2.

**Test Roof Attachment**

The fastening pattern for each of the four test roofs is shown in *Table 2*. For Tests #1, #2, and #3, purlin fasteners and 2½-in. barbed fastener plates were used to secure the membrane. The fasteners and plates were not stripped in. For Test #4, purlin fasteners and 3-in. TPO-coated, induction-welded fastener plates were used. The *Appendix* includes graphical representations of the fastening pattern for the four physical tests. For Tests #3 and #4, fasteners were staggered, meaning fasteners were offset one-half of the in-row spacing from row to row.

**PHYSICAL TESTING**

**Uplift Loading Pattern**

The physical testing was performed in accordance with the loading requirements for ASTM E1592 to determine wind uplift resistance for each test roof. Each test specimen was loaded to one-third of the nominal design pressure of the structural metal panel roof system, then the load was removed for three minutes. The specimens were then loaded with regular pressure steps of 7.2 psf until reaching 116.9 psf. After 116.9 psf, the steps were increased to 14.4 psf. Each pressure step was held for one minute of sustained pressure or until there was no increase in the deflection readings of the membrane under the given pressure. Three pressure sensors were mounted in the pressure chamber to monitor the actual pressure inside the chamber



*Figure 3 – The installed TPO for Test #2.*

| Test Roof # | Fastener Row Spacing, ft. | Fastener Spacing Within Each Row, in. | Fastening Method |
|-------------|---------------------------|---------------------------------------|------------------|
| 1           | 5                         | 12                                    | Above Membrane   |
| 2           | 5                         | 24                                    | Above Membrane   |
| 3           | 5                         | 36<br>(18 in. staggered)              | Above Membrane   |
| 4           | 5                         | 24<br>(12 in. staggered)              | Induction Welded |

*Table 2 – Test roof attachment layout for each roof assembly.*

during the testing. The three pressure sensors were located at the middle of the 10-ft. span in the transverse direction and at distances of 2 ft., 10 ft., and 18 ft., respectively, in the longitudinal direction. The pressure steps were continued on all

four roofs until failure occurred and pressure dropped.

Failure was either membrane rupture or fastener failure. This will be discussed in detail later in the paper. *Figure 4* shows the loading scheme defined by ASTM

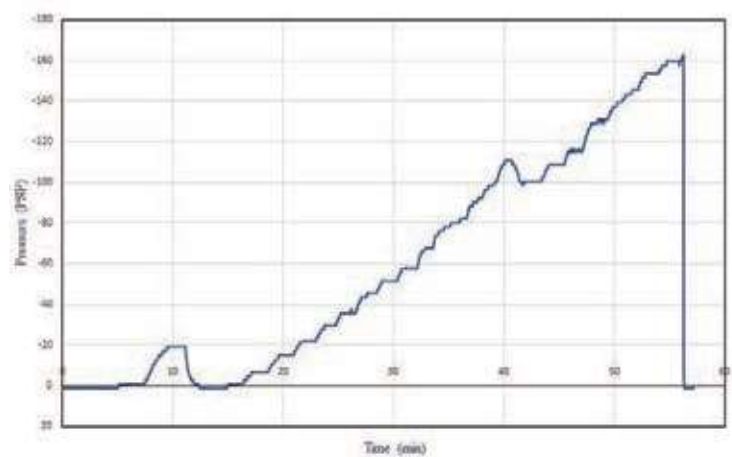
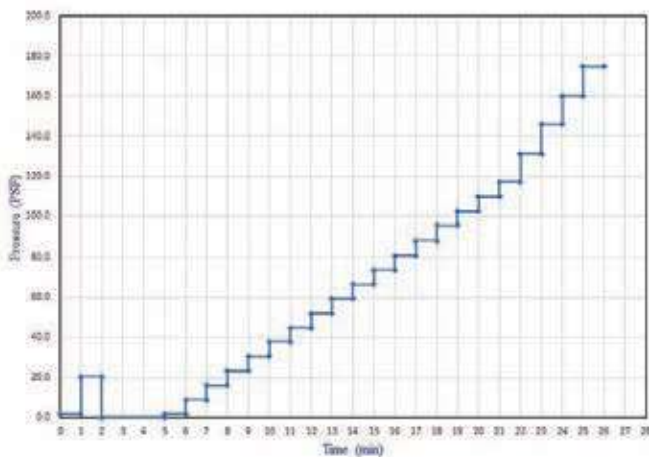


*Figure 4 – The loading scheme defined by ASTM E1592 and the actual loading scheme for Test #1.*

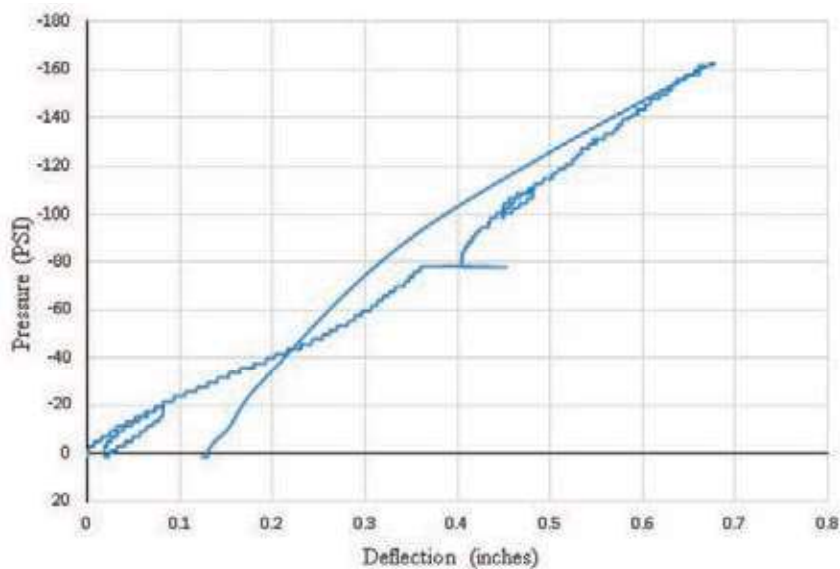
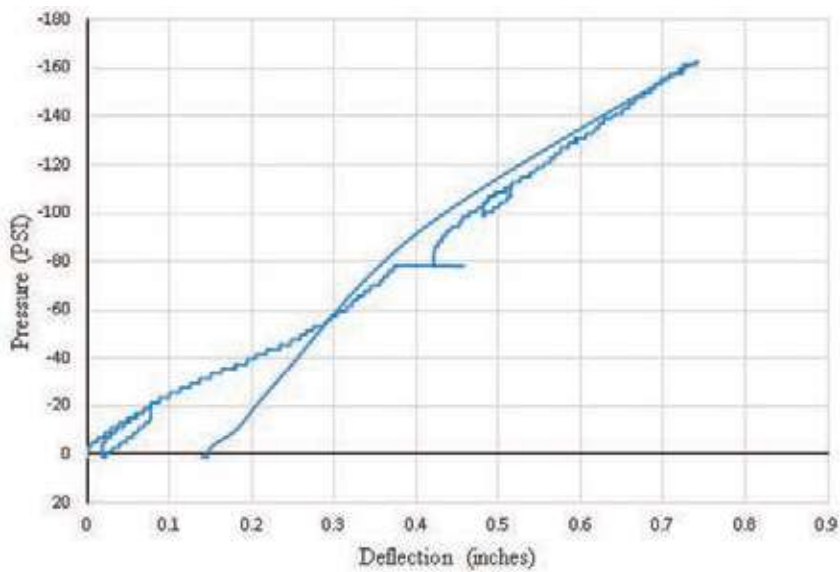
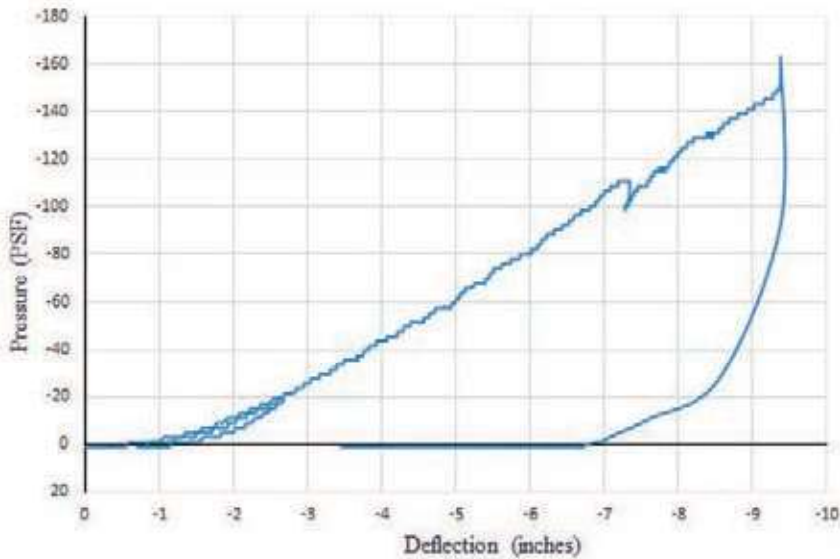


**Figure 5 – Applied pressure versus deflection for Test # 1: (a) membrane at mid-span between two rows of fasteners, (b) the screw for the metal panel clip, and (c) membrane fastener.**

E1592 used for testing and the actual loading scheme from Test #1.

### Data Collection

The underside of the deck and the interior of the chamber were heavily instrumented. The chamber included five video cameras, and there was an additional 360-degree camera in the center of the ceiling of the chamber.

Sensors were collecting data on:

- Strain of metal panel clips
- Strain and deflection of metal panels
- Displacement of expansion clip bolts
- Displacement of single-ply fasteners
- Upward displacement of membrane at center point between rows of fasteners
- Upward displacement of membrane fasteners
- Upward displacement of membrane between fasteners within the row
- Strain of the membrane adjacent to fastener plates

Figure 5 provides examples of the data collected during each test. These show the mid-span deflection of the membrane, the deflection of the screw for the metal panel clip, and the deflection of the membrane fastener at the middle purlin. The examples are from Test #1.

At the time of writing this paper, the data had not been formalized, but they will be provided at the 2020 IIBEC International Convention and Trade Show.

The purlins in all tests were attached to the C-channels with angles and bolts. This type of attachment did not allow for data collection at the purlin-to-mainframe connection, which is needed to assess the potential for overloading of the fastener at that connection. When an RSPRS is mechanically attached to every other purlin, the load path is altered significantly. This raises a question about the effect on the wind uplift capacity of the existing metal building when the load path is altered.<sup>5</sup> Therefore, it is recommended to engage a structural engineer when altering the load path of an existing structure.

## RESULTS AND DISCUSSION

### Uplift Results

Table 3 shows the ultimate loads achieved, tributary area, and load per fastener, as well as the fastening method. In this paper, the term “ultimate load” refers to the point of failure (or expected failure) of a roof system during physical testing.

### Test #1

The fastening pattern for Test #1 was 5-ft. o.c. fastener rows and 12-in. fastener spacing within the row. Test #1 failed when the membrane ruptured

| Test Roof # | Ultimate Load, <sup>a</sup> psf | Fastening Pattern             | Tributary Area per Fastener, <sup>b</sup> sf | Load per Fastener, lbs. | Fastening Method |
|-------------|---------------------------------|-------------------------------|--|-------------------------|------------------|
| 1           | 162.7 (160.1)                   | 5 ft. o.c. x 12 in.           | 5  | 813.5 (800)             | Above Membrane   |
| 2           | 119.5 (116.9)                   | 5 ft. o.c. x 24 in.           | 10   | 1195 (1160)             | Above Membrane   |
| 3           | 61.9 (59.3)                     | 5 ft. o.c. x 36 in. staggered | 15   | 928.5 (890)             | Above Membrane   |
| 4           | 64.8 (59.3)                     | 5 ft. o.c. x 24 in. staggered | 10   | 648 (593)               | Induction Welded |

Note a: Actual load recorded at time of failure is shown. The highest E1592 “step” successfully passed is shown parenthetically.

Note b: Tributary area and influence area may generally be used interchangeably when discussing the load acting on a specific fastener; tributary area is quickly calculable, while influence area is determined via physical testing.

**Table 3 – The ultimate loads, tributary area, and load per fastener for each test roof.**

simultaneously at seven fastener locations in the center purlin/row of fasteners. The system successfully completed 160.1 psf and then failed as the pressure was being increased to 174.5 psf. The membrane pulled over the five center fastener plate locations in an essentially circular pattern along the outer edges of the fastener plates. The outer two failure locations resulted in L-shaped tearing of the membrane, which was attributed to the boundary conditions of the test chamber. The fastener plates were deformed upward. There were many locations of permanent upward membrane deformation.

Figure 6 shows the outcome of Test #1.

The permanent upward membrane deformation was evident along the edges of the rows of fasteners, as can be seen in the upper row of fasteners in Figure 6. There was very little permanent upward membrane deformation at the centerline between fasteners within a row. This pattern of deformation leads to the belief that the load within the membrane is being transferred from fastener row to fastener row, and not significantly from fastener to fastener within a row. See Subsection “Test #3” for additional discussion.

### Test #2

The fastening pattern for Test #2 was 5-ft. o.c. fastener rows and 24-in. fastener spacing within the row. Test #2 failed when the membrane ruptured simultaneously at the three central fastener locations in the southern quarter-point row of fasteners. The system successfully completed 116.9 psf and then failed as the pressure was being increased to 124.1 psf. The membrane pulled over the three center fastener plate locations within the row. The center rupture was circular at the fastener plate. The outer two ruptures were D-shaped; the straight-line edges were attributed to the boundary conditions of the test chamber. Figure 7 shows the rupture at the center fastener plate from Test #2.

The tributary area for each fastener for Test #2 was double that of Test #1.



**Figure 6 – The outcome of Test #1. The membrane ruptured at the center row of fasteners. The outer two fastener locations where the membrane tore in an “L” shape are identified by red circles.**

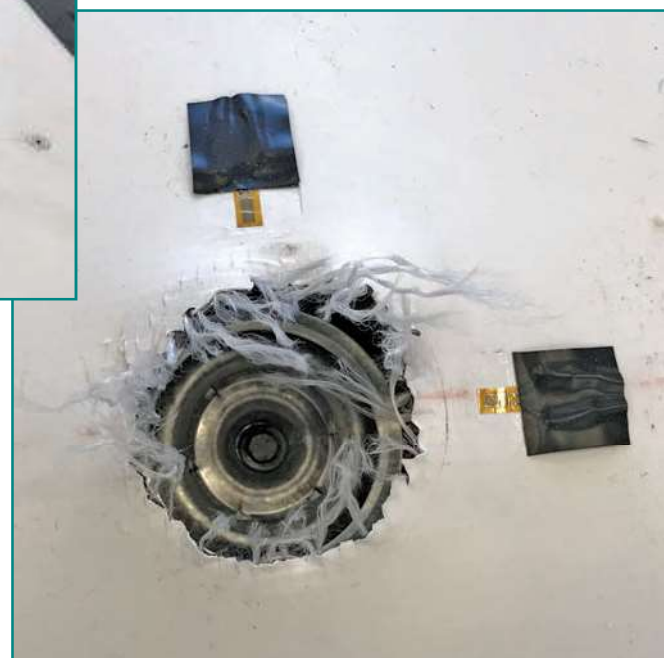


**Figure 7 – Membrane ruptures at the fastener plate locations for Test #2.**

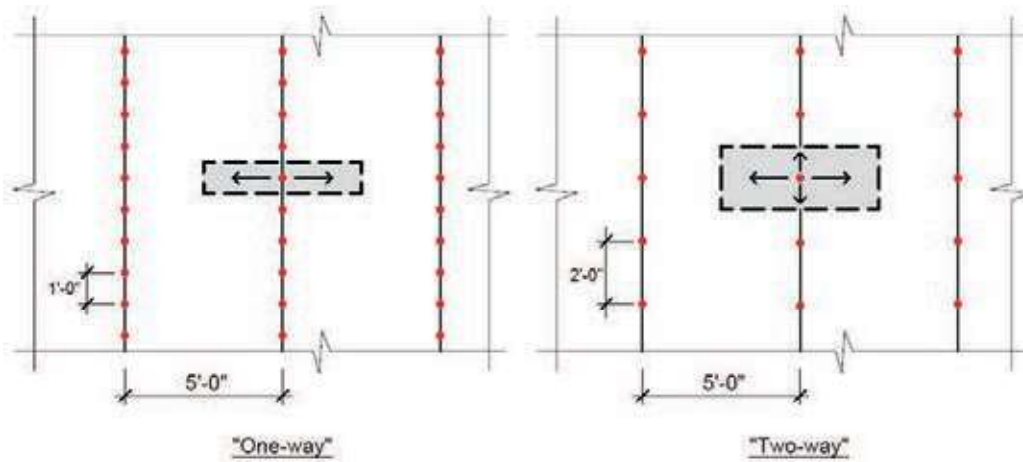


**Figure 8 – Graphical representation of one-way and two-way loading.**



**Figure 9 – Circular permanent upward membrane deformation due to two-directional loading in Test #2.**

This led to the assumption that the ultimate load for Test #2 would be one-half of that from Test #1, or 81.4 psf. However, the ultimate load was 119.5 psf, which is approximately 73% of that from Test #1. This is believed to indicate that the membrane transitioned from one-way loading to two-way loading, as shown in Figure 8.

The load path was not only distributed across the 5-ft. purlin-to-purlin span (as was the case in Test #1), but it was also distributed between fasteners within a row. The uplift loads were pulling on the fastener and fastener plates from all sides (two-way loading) instead of just two sides (one-way loading); during the test, the membrane deflected up approximately 4 in. between fasteners within a row. The loads were more equally distributed within the membrane and around the fastener plate, and therefore, the load per fastener increased from 813.5 to 1,195 lbs.



**Figure 10 – The failure location for Test #3, noted by the red circle.**

The membrane resisted the uplift loads in two generalized directions: between fastener rows and between fasteners within a row, which is in the same direction as the machine direction (MD) and cross-machine direction (XMD) reinforcement yarns within the membrane, respectively. The membrane had permanent upward membrane deformation between rows and between fasteners within a row because of this two-directional loading. The permanent upward membrane deformation was circular around fasteners, as seen in Figure 9. The circular membrane deformation indicates that load is being applied to the fastener from all directions, but to simplify the discussion, the term “two-way loading” is used.

### Test #3

The fastening pattern for Test #3 was 5-ft. o.c. fastener rows and 36-in. fastener spacing within the row; fasteners were staggered row to row. Test #3 failed when the membrane ruptured at a single fastener location in the southern quarter-point row of fasteners. The system successfully completed 59.3 psf and then failed as the pressure was being increased to 66.5 psf. The membrane pulled over the centermost fastener plate within the row, as shown in Figure 10.

Figure 11 shows a close-up of the failure location for Test #3. The failure was

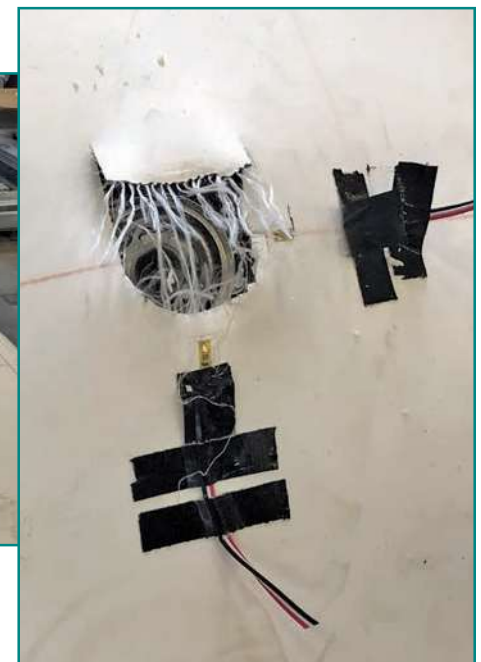


**Figure 11 – The failure location for Test #3.**



D-shaped, similar to failure locations in Test #2. The flat edge was on the boundary edge of the test roofs; the rounded edge was towards the center of the test roof.

Similar to Test #2, there was circular upward permanent membrane deformation at fastener locations for Test #3 as shown in *Figure 10*. This shows that the membrane is being loaded in the MD and XMD. This is due to the relatively wide spacing of the fasteners (2 ft. and 3 ft.) relative to Test #1, which had 1-ft. spacing of fasteners within a row.

The tributary area for each fastener for Test #3 was 50% greater than Test #2. This led to the assumption that the ultimate load would be two-thirds of Test #2, or about 79.7 psf. However, the ultimate load was 61.9 psf, which is approximately 52% of that from Test #2.

It was also assumed that staggering the fasteners between rows would increase the ultimate load. This assumption, at least for this test, was not accurate, given the above analysis.

Comparing Test #3 to Test #1, traditional assumptions based on tributary area would lead to an expected ultimate load for Test #3 to be one-third of Test #1. The ultimate load from Test #1 was 162.7 psf, so the expected ultimate load for Test #3 was 54.2 psf. The actual ultimate load for Test #3 was 61.9 psf, which is approximately 38% of that from Test #1.

While two-direction membrane loading appears to increase the expected ultimate load of a roof system relative to the traditional linear expectation of failure load, it appears there is a limit to this increase. For this series of tests, the limit seems



**Figure 13 – The top of an induction-welded fastener plate showing membrane delamination (cap to core separation).**

to be 5 ft. o.c. for fastener rows with 24-in. fastener spacing within each row.

#### Test #4

The fastening pattern for Test #4 was 5-ft. o.c. fastener rows and 24-in. fastener spacing within the row; fasteners were staggered row to row and induction welded. Test #4 failed in two locations when one fastener plate pulled over the fastener head and the membrane separated at the reinforcement layer at the adjacent welded fastener plate. The system successfully completed 59.3 psf and then failed as the pressure was being increased to 66.5 psf. The failures occurred in the southern quarter-point row of fasteners. *Figure 12* shows the failure locations for Test #4.

Test #4 used induction welding, which means the fastener plates were under the membrane. Therefore, the membrane was cut in order to evaluate each failure.

It was difficult to determine from visual examination which occurred first: the fastener plate pulling over the fastener head or the delamination of the membrane to the fastener plate. However, based on the loud noise that occurred at failure, it is believed that the fastener plate pulled over the fastener first and then load was immediately transferred to the adjacent fastener plate, causing the delamination.

Test #4 and Test #2 have the same tributary area per fastener location—10 ft.<sup>2</sup>. However, Test #2 achieved a 119.5 psf ultimate load, and Test #4 achieved a 64.8 psf ultimate load. All components were identical for both test roofs except for the fastener/plate combination and that Test



**Figure 12 – The two failure locations for Test #4. The double red circle is where the fastener plate pulled over the fastener; the single red circle is the location of the membrane separation at the reinforcement layer.**



It was difficult to determine from visual examination which occurred first: the fastener plate pulling over the fastener head or the delamination of the membrane to the fastener plate.



#4's fasteners were staggered row to row.

The above-membrane fastener (e.g., an in-seam fastener) is 2-3/8 inches in diameter. An induction-welded fastener plate is 3 inches in diameter and is constructed such that a "ring" adheres to the membrane, not the entire fastener plate. *Figure 13* shows this explicitly.

The area of a 2% in., above-membrane fastener plate is approximately 4.4 in.<sup>2</sup>. The area of the attachment surface for an induction-welded fastener plate is approximately 3.3 in.<sup>2</sup>. Therefore, an induction-welded fastener plate has approximately

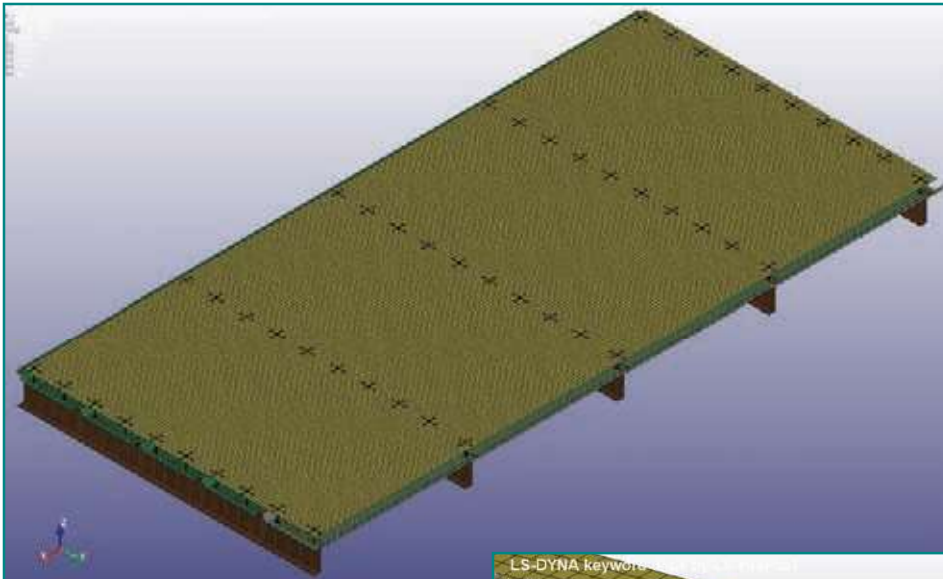


Figure 14 – Finite element modeling of RSPRS using LS-DYNA®.

75% of the area of an above-membrane (i.e., a traditional mechanically attached) fastener plate.

Individual fastener load for Test #2 (with the same tributary area as Test #4) was 1,195 lbs. Direct extrapolation to the induction-welded fastener plate (at 75%) leads to the assumption that the fastener load for Test #4 would be 896 lbs. This also assumes the reinforcement is the weak link, but the test clearly shows the cap-to-core connection (adhesion) is the weak link, and it therefore makes sense that the failure load per fastener for Test #4 was less than 896 lbs. In fact, it was 648 lbs. per fastener.

The analysis of these two different types of fastening methods and failure modes supports the result that Test #4 has lower wind uplift resistance than Test #2, even though the tributary area for each fastener is the same for Tests #2 and #4.

### FINITE ELEMENT ANALYSIS

Finite element (FE) modeling was carried out using LS-DYNA® software to investigate the behavior of the RSPRSs. The system was modeled using solid elements to be able to simulate the actual behavior of the roof system. Each RSPRS model was subjected to uniform negative pressure to simulate the wind uplift pressure. The FE models have the same dimensions and configuration as those of the tested RSPRSs. Different material models were selected for the steel members and the single-ply membrane to simulate accurate behavior of the roof. Detailed contact modeling between the fasteners and the pur-

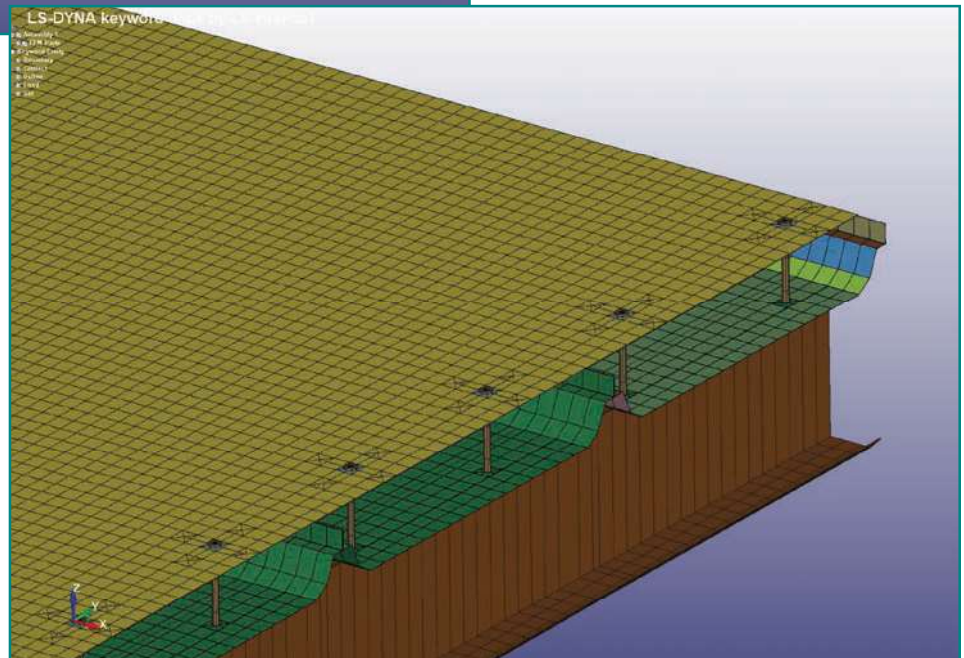


Figure 15 – Different element simulation of the RSPRS.

lins, as well as between the fasteners and single-ply membrane, is vital in this study to ensure accurate representation of the friction between different elements. Two types of contact were used in the modeling process: nodes-to-surface and surface-to-surface. Figure 14 shows the geometry of the simulated roof system in LS-DYNA. The connection between the metal panels and the purlins was also simulated to account for the deformation that occurred between the panels and the purlins. Figure 15 shows the configuration of the different elements considered in the FE model.

The models were validated with the experimental results from the tested roofs. Physical testing of an every-other type of RSPRS installation could not be performed due to physical limitations of the test chamber. However, FE modeling

will include simulation of the every-other installation type and is based on verified models from tests of large-scale roofs in order to be able to predict ultimate loads for the every-other installation type. This every-other installation type is of concern due to the unknown effect on the existing metal building's capacity to resist wind uplift when altering the load path.

### CONCLUSIONS AND RECOMMENDATIONS

Review and analysis of the four full-scale physical tests of retrofit single-ply roof systems installed over structural metal panel roof systems tested at MS&T resulted in a number of conclusions. They are as follows:

- Uplift resistance of RSPRSs and individual fastener loads in an

RSPRS are based on the membrane's reinforcement strength and one-directional versus two-directional loading of reinforcement.

- The failure modes for Tests #1, #2, and #3 were membrane ruptures at fastener locations. Specifically, the reinforcement was the point of failure for these tests.
- Two-directional membrane loading increases the expected ultimate load of a roof system relative to the linear extrapolation of an anticipated failure load at individual fasteners (which is commonly based on tributary area). However, it appears there is a limit to this expected increase. For this series of tests, the ultimate load exceeded expectations for the Test #2 fastening pattern, but the ultimate load was more in line with traditional linearly extrapolated expectations for the Test #3 fastening pattern.
- The roofing industry should take note of this information when determining uplift resistance of RSPRSs based on calculations. This work emphasizes the limitations of extrapolation and validates the use of physical testing to determine uplift resistance of roof systems.
- Permanent deformation of the membrane was observed in all four physical tests and was not seen to be a watertightness issue. Deformation and load were not correlated; however, this observation


may provide an explanation for “wrinkles” observed in mechanically attached membranes that have experienced high-wind events.

- Induction-welded systems rely on the heat-weld attachment of the membrane to the fastener plate. The failure mode for Test #4 was either the fastener plate pulling over the fastener head or membrane-to-fastener plate delamination.

### FUTURE WORK

The FE modeling of every-other installation types was not formalized at the time this paper was written. This information will be presented at the 2020 IIBEC International Convention and Trade Show.

There are additional research opportunities that stem from this work. They include:

- Do manufacturing tolerances for the membrane reinforcement and how the reinforcement is interfaced with the cap and core layers affect the ability for homogenous two-directional resistance to loads?
- From Test #4, which failure mode—induction-welded fastener plate pulling over the fastener or membrane delamination at induction-welded fastener plate—is the path of least resistance to failure? Small-scale tests can be performed to determine the comparative strength of each failure mode.
- Can FE modeling be used to predict uplift load capacity for RSPRSs that are fastened into the existing structural metal panels? 

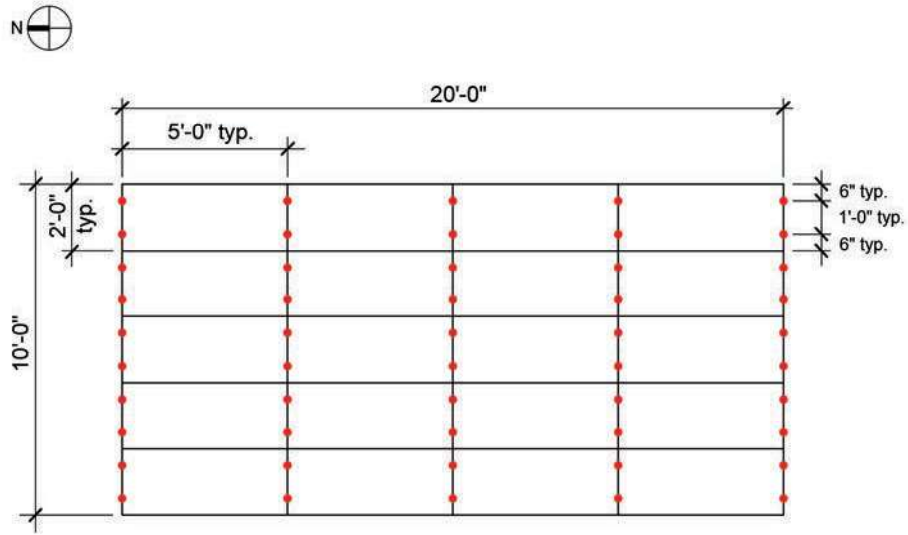
### ENDNOTES

1. This paper is the continuation of the study that was presented in March 2019 at the RCI (now IIBEC) Annual Convention and Trade Show in Orlando, FL, titled “Assessing Wind Resistance of Retrofit Single-Ply Roof Systems Installed over Existing Metal Panel Roof Systems.”
2. ASTM E1592-05 (2017), *Standard Test Method for Structural Performance of Sheet Metal Roof and Siding Systems by Uniform Static Air Pressure Difference*.
3. The Missouri University of Science and Technology's Civil, Architectural and Environmental Engineering Department is chaired by Joel Burken, PhD, PE, BCEE, FAESP. The work was directed by Mohamed ElGawady, PhD, professor and Benavides Faculty Scholar, with the assistance of PhD candidates. The lead PhD candidate was Yasser Darwish.
4. Missouri Builders Service, Inc., Post Office Box 104205, 3807 Route CC, Jefferson City, MO 65110. Phone: 573-636-7733. Web: [www.missouri-builders.net](http://www.missouri-builders.net).
5. James Kirby and Jennifer Keegan. “Assessing Wind Resistance of Retrofit Single-Ply Roof Systems Installed over Existing Metal Panel Roof Systems.” *Proceedings of the RCI [now IIBEC] International Convention and Trade Show*. March 14-19, 2019, Orlando.

# APPENDIX

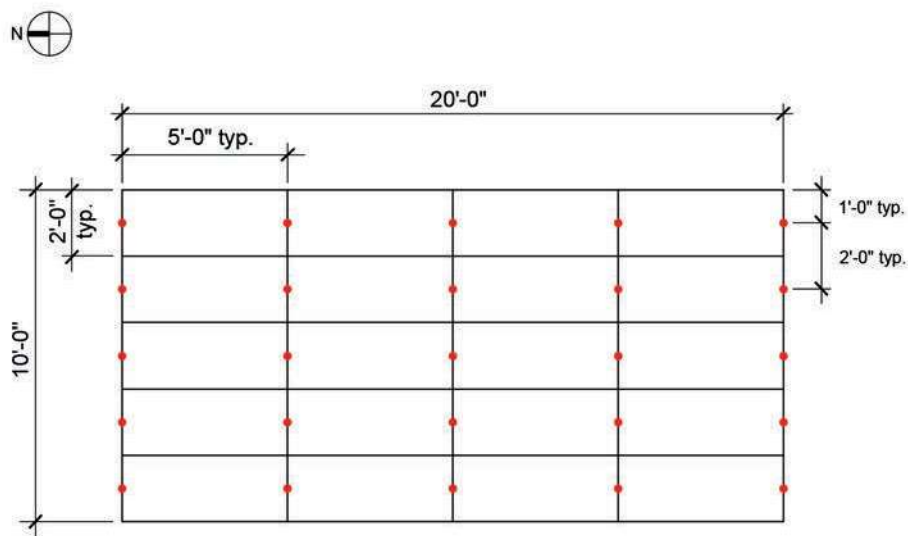
## FASTENING PATTERNS FOR PHYSICAL TESTS #1, #2, #3, AND #4

### Test #1: Fastener Pattern



Test #1 Fastener Pattern  
5'-0" o.c.; 12" in-row spacing

### Test #2: Fastener Pattern



Test #2 Fastener Pattern  
5'-0" o.c.; 24" in-row spacing

